PROPORTIONAL-DERIVATIVE LINEAR QUADRATIC REGULATOR CONTROLLER DESIGN FOR IMPROVED DIRECTIONAL AND LATERAL MOTION CONTROL OF UNMANNED AERIAL VEHICLES

by

YAP KAI WEN

Thesis submitted in fulfilment of the requirements for the Bachelor Degree of Engineering (Honours) (Aerospace Engineering)

June 2019

ENDORSEMENT

I, Yap Kai Wen hereby declare that I have checked and revised the whole draft of dissertation as required by my supervisor

(Signature of Student)

Date:

(Signature of Supervisor)

Name:
Date:

ENDORSEMENT

I, Yap Kai Wen hereby declare that all corrections and comments made by the supervisor and examiner have been taken consideration and rectified accordingly.

(Signature of Student)

Date:

(Signature of Supervisor)

Name:
Date:

(Signature of Examiner)

Name:
Date:

DECLARATION

This thesis is the result of my own investigation, except where otherwise stated and has not previously been accepted in substance for any degree and is not being concurrently submitted in candidature for any other degree.

(Signature of Student)

Date:

ACKNOWLEDGEMENTS

First and foremost, I must thank my final year project supervisor, Ir. Dr. Nurulasikin Mohd Suhadis. Without her assistance and dedicated involvement in every step throughout the process, this thesis paper would have never been accomplished. I would like to thank you very much for your support and understanding throughout the project period.

I would also like to show gratitude to my final year project examiner, Ir. Dr. Ahmad Faizul Hawary for his encouragement, insightful comments, and hard questions. His suggestions have aided me in approaching the final year project.

I thank my senior in Aerospace Engineering, Mr. Kok Kai Yit for the stimulating discussions. Also, I thank my friends in Universiti Sains Malaysia: Teo Chen Lung, Lim Yew Hao, Leong Yeong Chee, Lam Kuek Shen, Tan Chun Khuen, Low Jian Yan and Ng Kian Kiong.

Most importantly, none of this could have happened without my family. My father, who offered his encouragement through phone calls every week has become my moral support over the last several years. Every time I was ready to quit, he will always cheer me up and I am forever grateful. This thesis stands as a testament to your unconditional love and encouragement.

PROPORTIONAL-DERIVATIVE LINEAR QUADRATIC REGULATOR CONTROLLER DESIGN FOR IMPROVED DIRECTIONAL AND LATERAL MOTION CONTROL OF UNMANNED AERIAL VEHICLES

ABSTRACT

This study investigates the directional and lateral motion control of unmanned aerial vehicles by controlling the sideslip angle through a simulation in MATLAB/Simulink. The linear model of a mini unmanned aerial vehicle, Ultra Stick 25e is applied to controllers to explicate the lateral-directional motion of the unmanned aerial vehicle. Directional and lateral motion control of an unmanned aerial vehicle is very crucial especially when the unmanned aerial vehicle performs any maneuver. These maneuvers usually performed when the unmanned aerial vehicle is avoiding any flying obstacles or in tasks that require complex maneuvers. It is crucial for an unmanned aerial vehicle to have the ideal performance to achieve the desired response instantly with 100% precision especially when the unmanned aerial vehicle is avoiding flying obstacles. However, currently available controllers show a delay in the response time which need further improvements. Therefore, a proportional-derivative linear quadratic regulator controller is developed and compared with a proportional-integral-derivative controller, a linear quadratic regulator controller, and a proportional linear quadratic regulator controller. The flight condition of the mini unmanned aerial vehicle model was set at forward velocity, u=17m/s, pitch angle, θ= 0.0217rad, elevator deflection angle, η = 0.091rad, throttle angle, τ = 0.559rad, aileron and rudder deflections of ξ= 0rad, ζ= 0rad respectively, and altitude of 120m. The proportional-integral-derivative controller, linear

quadratic regulator controller, proportional linear quadratic regulator controller, and proportional-derivative linear quadratic regulator controller are simulated in MATLAB/Simulink and compared with the results in terms of rise time, settling time, overshoot, steady-state error and root mean square error. The tuning of each controller makes sure every controller performs at its optimized state which gives the best performance for each controller. The proportional-derivative linear quadratic regulator controller enhances the response of the system by reducing the settling time by more than 74% compared with other controllers. The rise time and steady-state error are improved by more than 50% whereas the root mean square error is improved by more than 6% and having the overshoot at a reasonable value.

KONTROLER PROPORSIONAL-DERIVATIF LINEAR KUADRATIK REGULATOR BAGI MENINGKATKAN KAWALAN PERGERAKAN BERARAH AND SISI KENDERAAN UDARA TANPA PEMANDU

ABSTRAK

Kajian ini menyiasat kawalan pergerakan berarah dan sisi kenderaan udara tanpa pemandu melalui simulasi dalam MATLAB / Simulink. Model linear kenderaan udara tanpa pemandu mini, Ultra Stick 25e digunakan oleh kontroler bagi mengutarakan usul sisi-arah kenderaan udara tanpa pemandu. Arah dan sisi kawalan pergerakan kenderaan udara tanpa pemandu adalah sangat penting terutamanya apabila kenderaan udara tanpa pemandu melaksanakan apa-apa manuver. Manuver-manuver ini biasanya dilakukan apabila kenderaan udara tanpa pemandu cuba mengelakkan sebarang halangan terbang atau dalam tugas-tugas yang memerlukan gerakan kompleks. Hal ini menjadi penting untuk kenderaan udara tanpa pemandu mempunyai prestasi yang ideal bagi mencapai output yang dikehendaki dengan serta-merta dan 100% ketepatan terutamanya apabila kenderaan udara tanpa pemandu sedang mengelakkan halangan terbang. Walau bagaimanapun, kontroler yang ada sekarang menunjukkan kelewatan dalam masa tindak balas yang memerlukan penambahbaikan. Jadi, kontroler proporsional-derivatif linear kuadratik regulator dikenalkan and disbanding dengan kontroler proporsional-integral-derivatif, kontroler linear kuadratik regulator, dan kontroler proporsional linear kuadratik regulator. Keadaan penerbangan model kenderaan udara tanpa pemandu mini telah ditetapkan pada halaju hadapan, u=17m/s, sudut padang, θ= 0.0217rad, pesongan sudut elevator, η = 0.091rad, sudut pendikit, τ = 0.559rad, pesongan aileron, ξ= 0rad, pesongan kemudi, ζ= 0rad, dan ketinggian dalam 120m. Kontroler proporsional-integral-derivatif, kontroler linear kuadratik regulator, kontroler proporsional linear kuadratik regulator,

dan kontroler proporsional-derivatif linear kuadratik regulator disimulasi dalam MATLAB / Simulink dan dibandingkan dengan keputusan dengan ‘rise time’, ‘settling time’, ‘overshoot’, ‘steady-state error’ dan ‘root mean square error’. Penalaan setiap kontroler memastikan setiap kontroler mampu mencapai tahap yang dioptimumkan untuk memberik prestasi yang terbaik bagi setiap kontroler. Kontroler proporsional-derivatif linear kuadratik regulator meningkatkan tindak balas sistem dengan mengurangkan ‘settling time’ dengan lebih daripada 74% berbanding dengan kontroler-kontroler lain. ‘Rise time’ dan ‘steady-state error’ telah ditambahbaik dengan lebih daripada 50% manakala ‘root mean square error’ telah ditambahbaik dengan lebih daripada 6% and kontroler mempunyai ‘overshoot’ dengan nilai yang munasabah.

TABLE OF CONTENTS

LIST OF FIGURES

LIST OF TABLES

LIST OF ABBREVIATIONS

UAV	Unmanned Aerial Vehicle
PID	Proportional-Derivative-Integral
LQR	Linear Quadratic Regulator
P-LQR	Proportional Linear Quadratic Regulator
PD-LQR	Proportional-Derivative Linear Quadratic Regulator
MAV	Micro Aerial Vehicle
RMSE	Root Mean Square Error
ARE	Algebraic Riccati Equation

LIST OF SYMBOLS

A	Wing Reference Area [m^2]
b	Wing Span [m]
$\bar{c}$	Wing Chord [m]
m	Gross Weight [kg]
m_C	Mass of Payload [kg]
m_T	Take-off Mass [kg]
I_x	Roll Moment of Inertia [kg.m^2]
I_y	Pitch Moment of Inertia [kg.m^2]
I_z	Yaw Moment of Inertia [kg.m^2]
I_{xz}	Product of Inertia [kg.m^2]
u	Forward Velocity [m/s]
θ	Pitch Angle [rad]
η	Elevator Deflection Angle [rad]
τ	Throttle Angle [rad]
ξ	Aileron Deflection [rad]
ζ	Rudder Deflection [rad]
β	Sideslip Angle [rad]
p	Roll Rate [rad/s]
r	Yaw Rate [rad/s]
ϕ	Roll Angle [rad]
l_v, l_p, l_r, l_ϕ	Rolling Moment
n_v, n_p, n_r, n_ϕ	Yawing Moment

y_v, y_p, y_r, y_ϕ	Dimensionless Stability Aerodynamic Derivatives
y_ξ , y_ζ	Dimensionless Control Aerodynamic Derivatives
Kp	Proportional Gain
Ki	Integral Gain
Kd	Derivative Gain
Td	Delay Time (s)
Tr	Rise Time (s)
Ts	Settling Time (s)
Tp	Peak Time (s)
Mp	Maximum Overshoot (%)

CHAPTER 1

INTRODUCTION

This chapter presents the problem faced in controlling the motion of Unmanned Aerial Vehicle (UAV) during its mission. The motion control of UAV is so important that it directly affects the success of a mission conducted. Poor motion control of UAV results in crashing of the UAV in mid-air, causing the failure of the mission. Therefore, controllers are used to improve the motion control of UAV and the success rate of a mission. In this thesis, a combination of Proportional-Derivative-Integral (PID) controller and Linear quadratic regulator (LQR) controller which is the Proportional-Derivative Linear Quadratic Regulator (PD-LQR) controller is introduced to improve the motion control of UAV.

1.1 Unmanned Aerial Vehicle (UAV)

UAV is an aircraft without a pilot aboard. It was originally implemented for military purpose to reduce risk and casualties of pilots in operations, but its involvement in civilian applications has grown rapidly recently. The civilian applications such as search and rescue (Półka & Kuziora, 2017), surveillance and reconnaissance, data collection and natural disaster response operations (Silva, De Mello & GOUVÊA, 2017) showed UAVs are widely been used. The UAV developed so rapidly due to its capability in reducing risk at low-cost. The presence of UAV benefits human in many ways other than reducing casualties in performing difficult tasks, but also improving the efficiency of a mission without requiring a large number of workforces. For example, the use of drone mapping improves the time efficiency compared to manual mapping which is way more significant when applying in the large test area (Eva, 2016).

1.2 UAV Motion Control

The UAV motion control can be separated into two groups, longitudinal motion control and lateral-directional motion control. The longitudinal motion control of UAV is responsible for controlling the pitching movement of the UAV whereas the lateral-directional motion control is to control the yawing and rolling movement of the UAV. In this study, the directional and lateral motion control of UAV will be focused on.

Directional and lateral motion control of UAV is very crucial especially when the UAV performs any maneuver. The directional and lateral stability ensure the UAV being stable during rolling or banking. These maneuvers usually performed when the UAV is avoiding any flying obstacles or in tasks that require complex maneuvers. Hence, the directional and lateral motion control always is an interesting study field because most UAV will not just be spending the whole time in longitudinal motion. Studies showed the design of directional and lateral controller used to control the directional and lateral motion of UAV (Swarnkar & Kothari, 2016), (Triputra et al., 2015). The studies used complete coupled six degrees of freedom model to simulate the motion control of UAV and showed the satisfactory performance of the overall architecture.

Sideslip angle is one of the state variables in the lateral state-space dynamics of UAV. In steady level flight, this angle must be controlled to ensure the lateral stability of the UAV. The large asymmetric aerodynamic loads induced on the fuselage of UAV when the UAV is at a high angle of attack produces side force and yawing moment. The UAV will eventually loss of control due to the directional and lateral instability caused by the asymmetric aerodynamic loads. This problem can be solved by controlling the sideslip angle to reduce the side force and yawing moment.

1.3 Problem Encountered in Existing Controllers

The ideal performance of a UAV is to have an instant response over the pilot's command with 100% precision. However, in real case, the communication link between the UAV and the ground control existing time delay and errors which prevent the pilot to have full and precise real-time motion control on UAV. Therefore, computational algorithms, such as PID, LQR, fuzzy logic, and neural network, have been studied to aid in stabilizing the UAV (Liu et al., 2017). PID and LQR controllers are widely used in controlling the motion of UAV while the combination of both controllers is less implemented. Since PD-LQR controller showed an overall improvement in longitudinal motion control of UAV, therefore the same controller is predicted to have same improvement in directional and lateral motion control of UAV.

1.4 Objective

The objectives of the project are:

i. To improve the directional and lateral motion control of UAV in controlling the sideslip angle using PD-LQR controller by reducing the rise time, settling time, overshoot, steady-state error and RMSE.

ii. To investigate and compare the performance PID controller, LQR controller, P-LQR controller and PD-LQR controller in terms of their step response characteristics.

CHAPTER 2

LITERATURE REVIEW

This chapter presents the review of literature relates to the motion control of UAV using various control algorithms. Some literature shows the improvement in the motion control of UAV on a large scale.

2.1 UAV motion control using PID controller

PID controller is a commonly used controller in researching on UAV stability control (Haoqin et al., 2015). This controller is good to enhance the response times of systems with first- or second-order characteristics. The PID controller is popular because its simple structure can be easily applied with sufficient performance. The fault-tolerant control of fixed-wing UAV in the presence of actuator failure has been investigated. The inclusion of a PID control architecture in the longitudinal and lateral control system gives the advantage to detect which control surface has failed and redistribute the required control effort and the effectiveness of the control methodology is guaranteed (Pedro & Tshabalala, 2017).

2.2 UAV motion control using LQR controller

LQR controller is known for minimizing cost function, which the LQR algorithm reducing the amount of time for control system engineer to optimize the controller. A Study has been done on integral LQR controller for inner control loop design of a fixed-wing Micro Aerial Vehicle (MAV). The adding integral action to the LQR inner loop controller in traditional PID controller displays a better dynamic performance in terms of transition time and speed overshoot and stronger robustness of LQR control methodology than that of traditional PID controller (Anjali et al., 2016). A control system

is designed on the (Lapan Surveillance UAV-05) LSU-05 to fly steadily using LQR controller. Based on LQR controller, the obtained transient response for longitudinal motion, delay time, td = 0.221s, rise time, tr = 0.419s, settling time, ts = 0.719s, peak time, tp = 1.359s, and maximum overshoot, Mp = 0%. In other hand, transient response for lateral-directional motion showed that td = 0.186s, tr = 0.515s, ts = 0.87s, tp = 2.02s, and Mp = 0% (Purnawan & Purwanto, 2017). Another study has investigated on a conventional integral LQR controller for the lateral-directional dynamics. Simulations show good performances of the overall architecture (Gavilan et al., 2015).

2.3 Improvement of UAV motion control using P-LQR controller

The results in controlling the UAV motion using PID controller and LQR controller are good but still can be improved. An improvement has done by combining the two control algorithms into one which becomes the P-LQR controller. The behaviour of increasing the proportional gain to reduce the response time of the system was implemented in the LQR controller. Results show that P-LQR controller has significantly improved the response times of the control system by at least 38.55% compared with other existing controllers (Kok & Rajendran, 2015). The downside of this controller is the increase in overshoot which causes the system more likely to become unstable.

2.4 Improvement of UAV longitudinal motion control using PD-LQR controller

Research has been done on PD-LQR controller for improved longitudinal motion of UAV. PD-LQR controller is the combination of both PID and LQR controllers which keeps the original advantage of each controller while improving the results even better. The use of PD-LQR controller has improved the overall response of the system by reducing settling time by more than 95% compared with PID, LQR and P-LQR controllers. It also improves the root mean square error (RMSE) by almost 50%

compared with the P-LQR controller and improves rise time by almost 96% with reasonable overshoot (Kok et al., 2016). However, the implement of PD-LQR controller is not yet proven to be effective for improving directional and lateral motion of UAV raised an interest to be found out.

2.5 Literature Gap

There are many kinds of research done in improving the motion control of UAV using various type of controller. Among the controllers, the combination of PID controller and LQR controller which is PD-LQR controller shows an outstanding result in improving the longitudinal motion control of UAV. However, it is still unknown that if this new proposed controller can also apply in the directional and lateral motion control of UAV. Study shows that LQR controller gives a good result in terms of the time response in lateral-directional motion control of UAV, but it is still not considered as instant response which improvement is still available. Since the PD-LQR controller shows the improvement in longitudinal motion control of UAV by reducing the settling time more than 95%, it is proposed here to improve the directional and lateral motion of UAV.

CHAPTER 3

METHODOLOGY

This chapter presents the mathematical model of UAV lateral-directional dynamics used in the designing of the control algorithms. The mathematical model acquired in state-space form and transfer function form. Besides, the development and the tuning process of each control algorithm will be discussed in detail with figures.

3.1 Mathematical Modelling

A mini-UAV, Ultra Stick 25e is chosen in this investigation on lateral-directional motion control. The Ultra Stick 25e is fixed-wing, radio controlled and equipped with conventional elevator, aileron and rudder as control surfaces. The UAV is assumed to be symmetrical where the effects of the cross-coupling are assumed negligible on the yaw-roll motion (Aliyu et al., 2016). The physical characteristics of the UAV are listed in Table 3.1.

Table 3.1: UAV parameters

Parameter	Description	Value
A	Wing Reference Area	$0.31\ m^2$
b	Wing Span	$1.27\ m$
$\bar{c}$	Wing Chord	$0.25\ m$
m	Gross Weight	$1.9\ kg$
m_C	Mass of Payload	$0.25\ kg$
m_T	Take-off Mass	$2.15\ kg$
I_x	Roll Moment of Inertia	$0.07151\ kg.m^2$
I_y	Pitch Moment of Inertia	$0.08636\ kg.m^2$
I_z	Yaw Moment of Inertia	$0.15364\ kg.m^2$
I_{xz}	Product of Inertia	$0.014\ kg.m^2$

The UAV is linearized at altitude of 120m and forward velocity, $u = 17m/s$, pitch angle, $\theta = 0.0217rad$, elevator deflection angle, $\eta = 0.091rad$, throttle angle, $\tau = 0.559rad$, aileron and rudder deflections of $\xi = 0rad$, $\zeta = 0rad$ respectively. Two assumptions are made to decouple the linear model. The assumptions are:

- The conventional control surfaces in the UAV design will not give significant cross-coupling control between the lateral-directional and longitudinal modes.
- The inertia cross coupling in xy (lateral) and xz (longitudinal) planes results in minimal cross-coupling between lateral and longitudinal modes as the UAV is symmetrical about the xz plane.

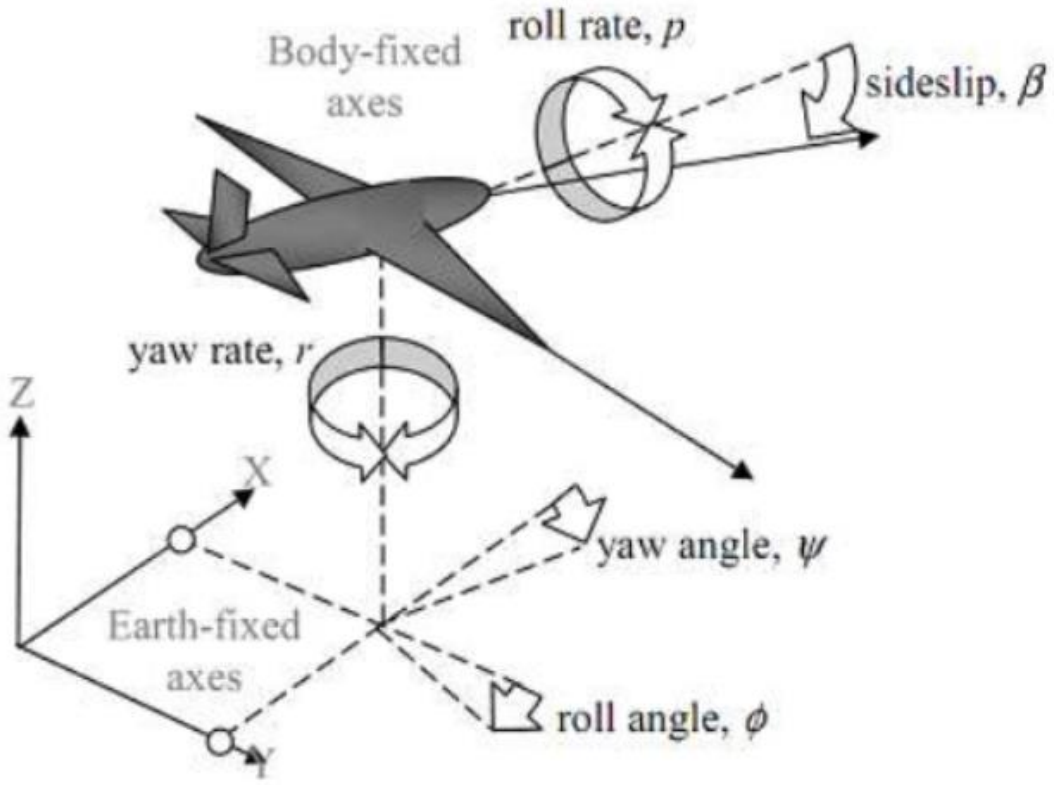

Figure 3.1: Perturbed lateral-directional dynamics of UAV (Aliyu et al., 2016).

Figure 3.1 shows the perturbed lateral-directional dynamics of UAV. The state-space equation is modified to incorporate sideslip angle, β. The equation is obtained through the linearization and expressed in following:

$$\begin{bmatrix}\dot{\beta}\\ \dot{p}\\ \dot{r}\\ \dot{\phi}\end{bmatrix}=\begin{bmatrix}y_v & y_p/V_0 & y_r/V_0 & y_\phi/V_0\\ l_vV_0 & l_p & l_r & l_\phi\\ n_vV_0 & n_p & n_r & n_\phi\\ 0 & 1 & 0 & 0\end{bmatrix}\begin{bmatrix}\beta\\ p\\ r\\ \phi\end{bmatrix}+\begin{bmatrix}y_\xi/V_0 & y_\zeta/V_0\\ l_\xi & l_\zeta\\ n_\xi & n_\zeta\\ 0 & 0\end{bmatrix}\begin{bmatrix}\xi\\ \zeta\end{bmatrix} \quad (1)$$

Where β is the sideslip angle, p is the roll rate, r is the yaw rate, ϕ is the roll angle, l_v, l_p, l_r and l_ϕ are the rolling moments with respect to the state variables, n_v, n_p, n_r and $n_\phi$are the yawing moment with respect to the state variables, y_v, y_p, y_r and y_ϕ are the dimensionless stability aerodynamic derivatives with respect to the state variables, y_ξ and y_ζ are the dimensionless control aerodynamic derivatives, ξ and ξ are the aileron and rudder input control signal. The state-space model in this study is:

$$\dot{x}=\begin{bmatrix}-0.86 & 0.93 & -16.76 & 9.69\\ -2.76 & -15.83 & 3.31 & 0\\ 1.67 & 0.51 & -2.73 & 0\\ 0 & 1 & 0.07 & 0\end{bmatrix}x+\begin{bmatrix}0.05 & 5.12\\ -154 & -4.93\\ 11.30 & -80.70\\ 0 & 0\end{bmatrix}\begin{bmatrix}\xi\\ \zeta\end{bmatrix} \quad (2)$$

$$y=\begin{bmatrix}0.59 & 0 & 0 & 0\end{bmatrix}\begin{bmatrix}\beta\\ p\\ r\\ \phi\end{bmatrix} \quad (3)$$

The transfer functions of the lateral-directional motion are obtained using the MATLAB command *ss2tf*. There are two transfer functions where equation (4) shows the inputs from aileron and equation (5) shows the inputs from rudder.

$$G(s)_{\beta\xi}=\frac{0.0295s^3-195.6912s^2-2077.0397s-2149.5911}{s^4+19.42s^3+88.0454s^2+482.6698s+2.4720} \quad (4)$$

$$G(s)_{\beta\zeta}=\frac{3.0208s^3+851.3548s^2+12568.1195s-2116.3308}{s^4+19.42s^3+88.0454s^2+482.6698s+2.4720} \quad (5)$$

3.3 Performance Indices

The performance indices must be determined to make sure that all parameters obtained by the newly designed controller algorithm are usable. To do so, the response of the system should have the overshoot with less than 10% and the control precision should be lower than ±1 %. Moreover, the ideal performance for rise time, settling time, overshoot, steady-state error, and root mean square error (RMSE) should be close to zero as much as possible. Since the model is a mini UAV, the expected level of precision should be ±0.001s (Kocer et al., 2019).

3.2 Design of Controllers

There are total four control algorithms developed in this study which are PID, LQR, P-LQR and PD-LQR to control the lateral-directional motion of the UAV. Simulink is used in designing control algorithms (Martyanov et al.,2015).

3.2.1 PID Controller

PID controller is a commonly used controller in researching on UAV stability control. This controller is good to enhance the response times of systems with first- or second-order characteristics. It involves three gain values which are proportional, derivative and integral. The equation of PID controller is expressed as below (Abdelhay & Zakriti, 2019):

$$u(t) = K_p e(t) + K \int_0^t e(\tau) d\tau + K_d \frac{de(t)}{dt} \quad (6)$$

The design of the PID controller circuit involves the transfer function of the lateral-directional motion. The overall flow of a PID controller is shown in Figure 3.2.

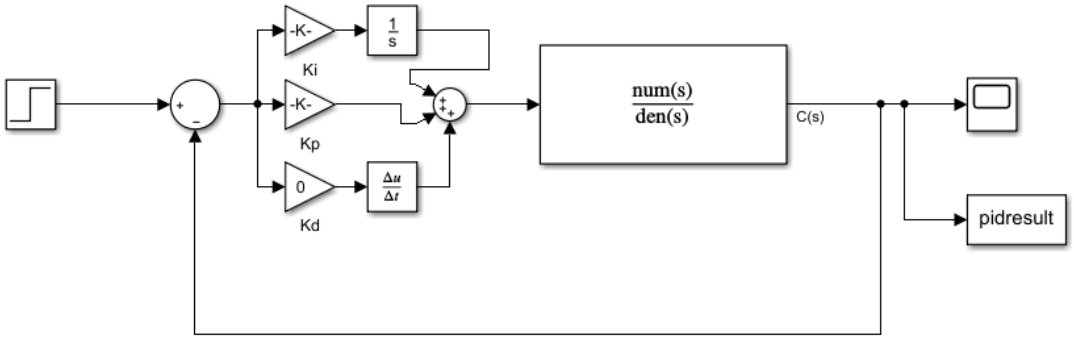

Figure 3.2: The flow of PID controller.

3.2.2 LQR Controller

LQR is an optimal control technique applied in a closed-loop system. It provides practical feedback gains to achieve the best performance. The objective of LQR is to design a state feedback controller K that control the difference between the output of the system with the desired value. The system equation can be expressed as follow (Kudinov et al., 2019):

$$\dot{x} = Ax + Bu \tag{7}$$

The system comes with a cost function as

$$J = \int_0^\infty (x^T Q x + u^T R u) dt \tag{8}$$

Where Q and R are weight matrices. Q is positive definite or positive semi-definite symmetry matrix whereas R is positive definite symmetry matrix. The cost function J need to be minimized to obtain an optimal control signal. A large Q required a low system state $x(t)$ to keep the cost function J small while a large R required a low control input $u(t)$ to keep the cost function J small (Vinodh & Jerome, 2013). The optimum control vector for the state space form is given by

$$u = -Kx \tag{9}$$

Where *K* can be obtained through

$$K = R^{-1}B^{T}P \tag{10}$$

P is found by solving the continuous time Algebraic Riccati Equation (ARE) (Gandhi et al., 2017) and substituted in equation (10).

$$A^{T}P + PA + Q - PBR^{-1}B^{T}P = 0 \tag{11}$$

The design of LQR controller requires the state matrices from equation (2) and (3), the flow of the controller is shown is Figure 3.3.

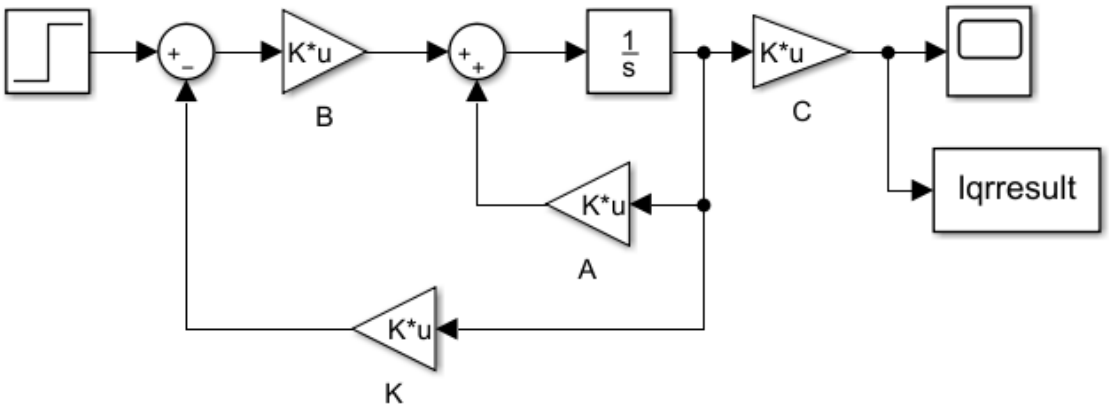

Figure 3.3: The flow of LQR controller.

3.2.3 P-LQR Controller

The idea of combining the PID controller and LQR controller to have a new control algorithm that keeps the advantages from both controllers is introduced which is P-LQR controller. The LQR controller has given the optimum control to the system is now added with another closed loop as negative feedback in the LQR controller, making the system response as additional system feedback. The closed loop will function as a

proportional controller when a gain parameter is added. However, another gain parameter is needed to balance the desired response due to the additional system feedback. Since the controller is modified by adding only proportional gain, therefore the P stands for proportional in the P-LQR controller (Kok & Rajendran, 2015). The overall flow of the P-LQR controller is shown in Figure 3.4.

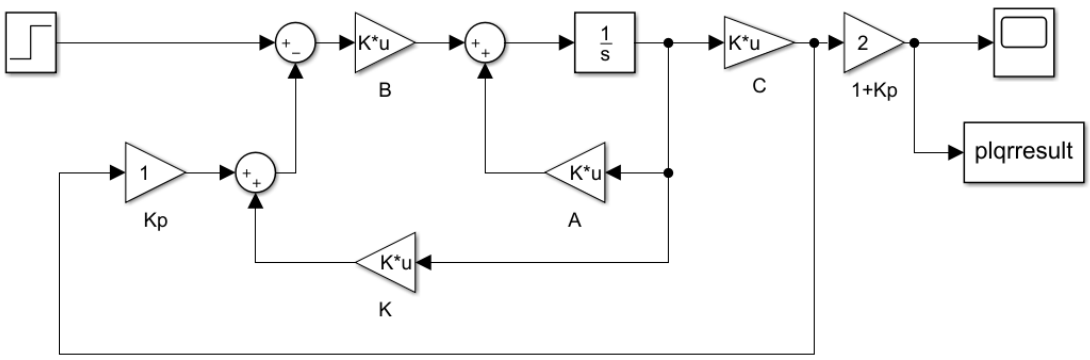

Figure 3.4: The flow of P-LQR controller.

3.2.4 PD-LQR Controller

The addition of proportional gain in the LQR controller did increase the response speed of the controller, but it also brings an undesired problem to the controller which is the increase of the overshoot. This increase in overshoot will make the controller become more unstable than before. Therefore, a derivative controller element is added in P-LQR controller to overcome the overshoot problem and make the response smoother. With the addition of the derivative gain in the controller, the controller is now named as PD-LQR controller where the D stands for derivative (Kok et al., 2016). The overall flow of PD-LQR controller is shown in Figure 3.5.

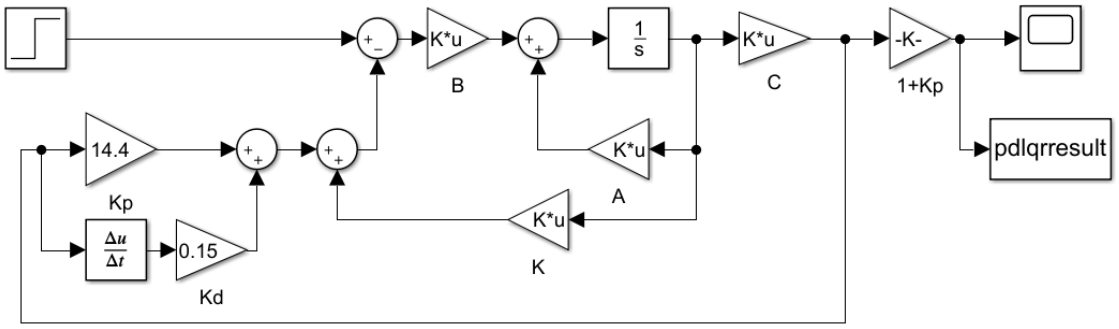

Figure 3.5: The flow of PD-LQR controller.

3.3 Tuning of Controllers

A controller proves no use if it is not tuned to get its optimal gain value for the system. Different controllers have different tuning method to obtain the optimal gain. In the tuning of these four controllers, MATLAB, Simulink and Microsoft Excel are being used.

3.3.1 PID Controller

The tuning of PID controller is much simpler with the aid from MATLAB. The built-in PID Tuner in the MATLAB requires only the transfer function of the system and the software will autotune the transfer function with the selected combination of proportional control, integral control and derivative control. Based on the autotune result, the optimal gain for the PID controller is shown in Table 3.2.

Table 3.2: Optimal gain values for PID controller

Transfer Function	Aileron Input	Rudder Input
Kp	-0.0199	-0.00307
Ki	-0.0002	-0.00001
Kd	0	0

A PID controller is developed in Simulink to verify the autotune result. The step-response characteristics of the controller are obtained using the *stepinfo* command in MATLAB and the steady state error of the controller is calculated in MATLAB as well.

3.3.2 LQR Controller

The tuning of LQR is to adjust the suitable weight matrices *Q* and *R* to get the optimal gain matrix *K* (Nagarkar et al., 2018). The state matrices *A, B, C* and *D* can be obtained from the state-space model of lateral-directional dynamics such that:

$$A = \begin{bmatrix} -0.86 & 0.93 & -16.76 & 9.69 \\ -2.76 & -15.83 & 3.31 & 0 \\ 1.67 & 0.51 & -2.73 & 0 \\ 0 & 1 & 0.07 & 0 \end{bmatrix} \tag{12}$$

$$B = \begin{bmatrix} 0.05 & 5.12 \\ -154 & -4.93 \\ 11.30 & -80.70 \\ 0 & 0 \end{bmatrix} \tag{13}$$

$$C = \begin{bmatrix} 0.59 & 0 & 0 & 0 \end{bmatrix} \tag{14}$$

$$D = 0 \tag{15}$$

To find the optimal feedback gain matrix *K*, *P* must be found in the ARE as in equation (11). Then, substitute value *P* into equation (10) to obtain the optimal feedback gain matrix *K*. The optimal feedback gain matrix *K* can be obtained using the MATLAB command *lqr(A,B,Q,R,N).* Table 3.3 shows the value of weight matrices and the optimal feedback gain matrix.

Table 3.3: Value of weight matrices and the optimal feedback gain matrix

Matrices	Value
Q	$\begin{bmatrix} 0.245 & 0 & 0 & 0 \\ 0 & 1 & 0 & 0 \\ 0 & 0 & 0.08 & 0 \\ 0 & 0 & 0 & 500 \end{bmatrix}$
R	$\begin{bmatrix} 1 & 0 \\ 0 & 1 \end{bmatrix}$
K	$\begin{bmatrix} -0.0491 & -1.0359 & -0.0164 & -22.1757 \\ 0.4505 & -0.0740 & -0.4636 & -2.9519 \end{bmatrix}$

3.3.3 P-LQR Controller

The P-LQR controller's performance varies when the percentage of response added as negative feedback. The proportional gain value is varied between 0 to 1 as the increment of the percentage of response added as negative feedback from 0% to 100%. Figure 3.6, Figure 3.9 and Figure 3.10 show the rise time, RMSE and steady-state error decrease as the percentage of response added as negative feedback increases and reach minimum at 100%. Figure 3.7 shows the settling time increases from 0% to 10% increase in the percentage of response added as negative feedback, then decreases as the percentage of response added as negative feedback increases. Figure 3.8 shows the overshoot of the system response increases almost linearly as the percentage of response added as negative feedback increases.

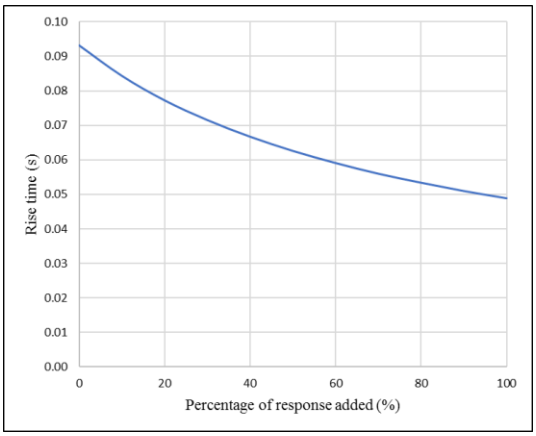

Figure 3.6: Change in rise time with gain variation in P-LQR controller

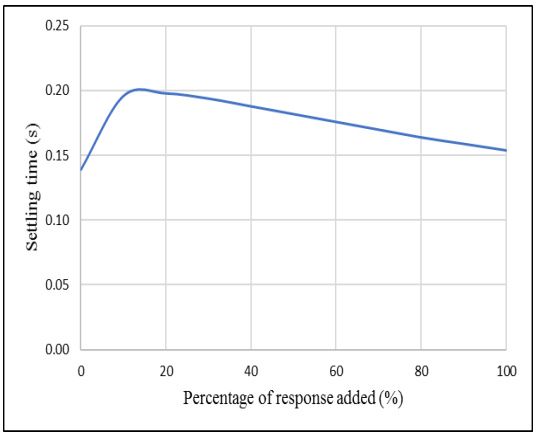

Figure 3.7: Change in settling time with gain variation in P-LQR controller

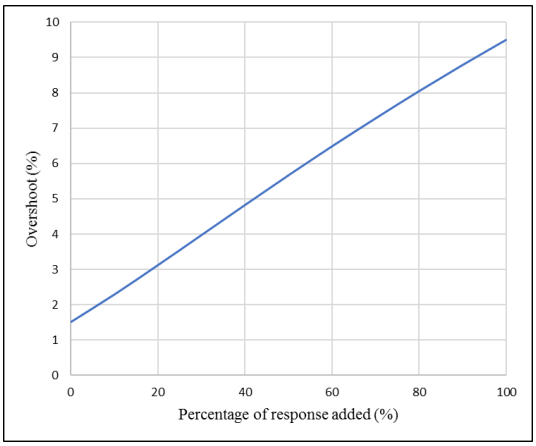

Figure 3.8: Change in overshoot with gain variation in P-LQR controller

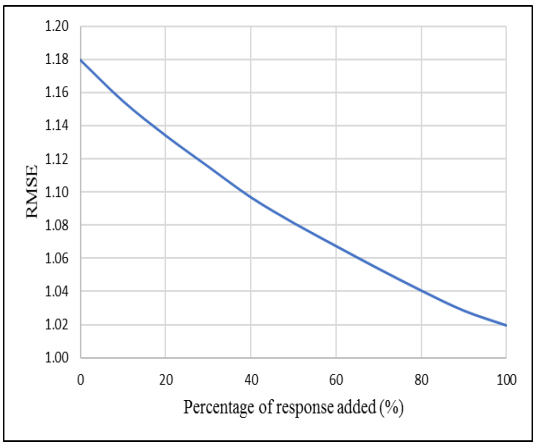

Figure 3.9: Change in RMSE with gain variation in P-LQR controller

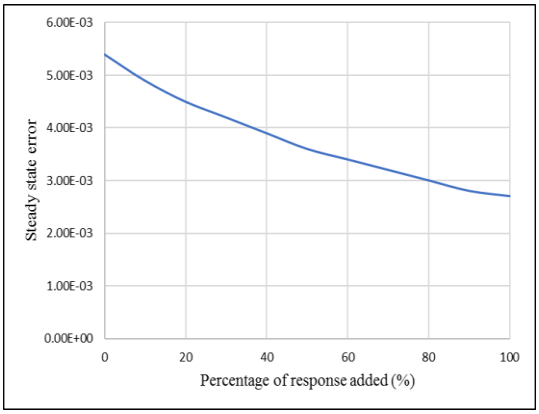

Figure 3.10: Change in steady-state error with gain variation in P-LQR controller

Table 3.4: Change in step-response characteristics with gain variation in P-LQR controller

Percentage of response added (%)	Rise time (s)	Settling time (s)	Overshoot (%)	RMSE	Steady State Error
0	0.093	0.139	1.510	1.179	5.40E-03
10	0.084	0.196	2.290	1.155	4.90E-03
20	0.077	0.198	3.120	1.134	4.50E-03
30	0.072	0.194	3.970	1.115	4.20E-03
40	0.067	0.188	4.820	1.097	3.90E-03
50	0.063	0.182	5.660	1.081	3.60E-03
60	0.059	0.176	6.480	1.067	3.40E-03
70	0.056	0.170	7.270	1.054	3.20E-03
80	0.053	0.164	8.040	1.041	3.00E-03
90	0.051	0.159	8.780	1.028	2.80E-03
100	**0.049**	**0.154**	**9.490**	**1.020**	**2.70E-03**

Table 3.4 shows the change in step-response characteristic of the system with the variation in proportional gain value. The set data with 100% of response added as negative feedback gives the best performance in overall since it has the smallest rise time, RMSE and steady-state error, a good performance in settling time while the overshoot of the system is still within 10%. Therefore, the optimal Kp value in P-LQR controller is 1.

3.3.4 PD-LQR Controller

In the previous controller which is P-LQR controller, the increase in proportional gain did results in improving the response time of the system but the con is the increase in overshoot. A high value of overshoot tends to make the system becomes unstable. Therefore, there is a limit in adding the proportional gain value to the P-LQR controller. However, this problem can be solved by using the proposed control algorithm which is PD-LQR controller. The purpose of derivative gain in this controller is like a booster for the system which reduces the overshoot and enables the limit on the proportional gain goes higher.

Increment of Proportional Gain in PD-LQR

The following figures show the increment of proportional gain without any derivative gain. Figure 3.11, Figure 3.12, Figure 3.14 and Figure 3.15 show that the rise time, settling time, RMSE and steady-state error decrease as the proportional gain increases. The results are good since the response time and the system errors have been improved a lot, but Figure 3.13 shows the overshoot of the system starts to overwhelm as the proportional gain increases. The improvements in the response time and the system errors become unpractical since the overshoot is exceeded 10%.

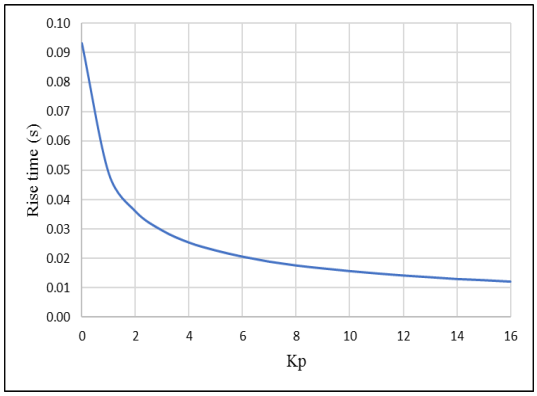

Figure 3.11: Rise time along proportional gain

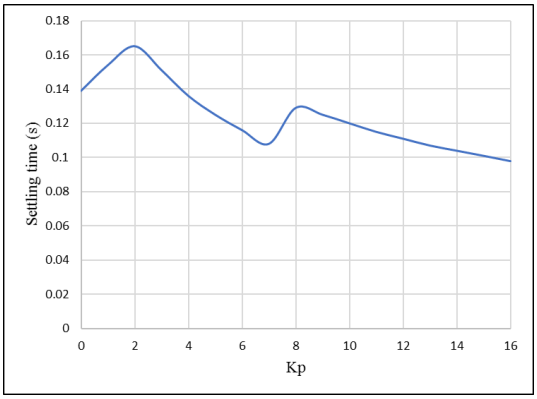

Figure 3.12: Settling time along proportional gain

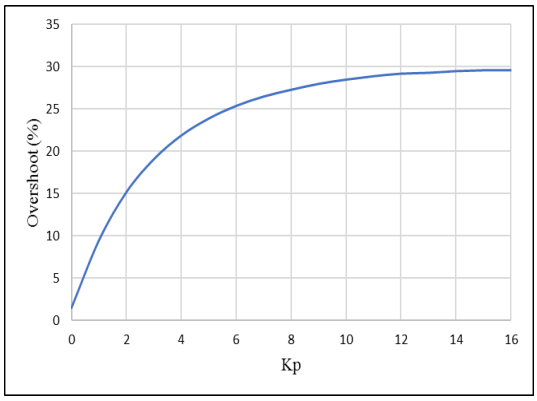

Figure 3.13: Overshoot along proportional gain

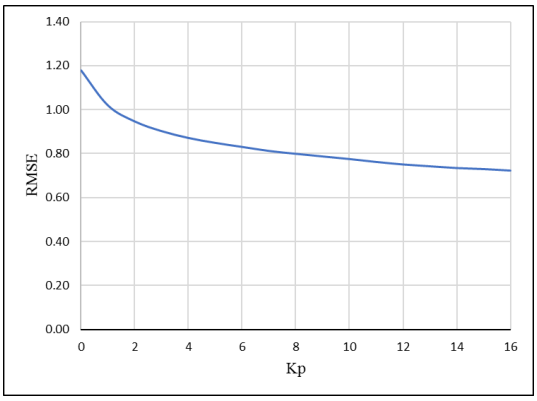

Figure 3.14: RMSE along proportional gain

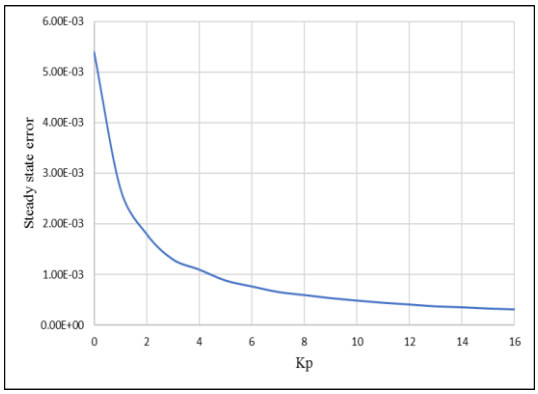

Figure 3.15: Steady-state error along proportional gain

Increment of Derivative Gain for Particular Gain in PD-LQR

Any proportional gain value can be optimized with a suitable derivative gain value. The derivative gain will bring down the overshoot of the system drastically but still having a good performance in rise time, settling time, RMSE and steady-state error. The limit of the derivative gain in this system is 0.65. The Simulink model cannot solve the simulation if the derivative gain goes beyond the limit. Figure 3.18 shows the increment of the derivative gain reduces the overshoot to nearly zero which completely solved the problem faced in P-LQR controller. Figure 3.16 and Figure 3.19 show the rise time and RMSE increase as the derivative gain increases. Therefore, both the parameters are not the deciding parameter in determining the best derivative gain for the particular proportional gain. Figure 3.17 shows the settling time of the system experienced a decreasing gradient and increase gradient as the derivative gain increases. Along the increment of the derivative gain, there is a minimum point for the settling time of the system which happens at derivative gain of 0.15. The steady-state error of the system fluctuates when the derivative gain increases as shown in Figure 3.20. Although the steady-state error is fluctuating, the minimum point happens same as where the minimum point of the settling time happens which is at a derivative gain of 0.15. Hence, the

deciding parameters to determine which derivative gain is the best value for the particular proportional gain is the settling time and the steady-state error.

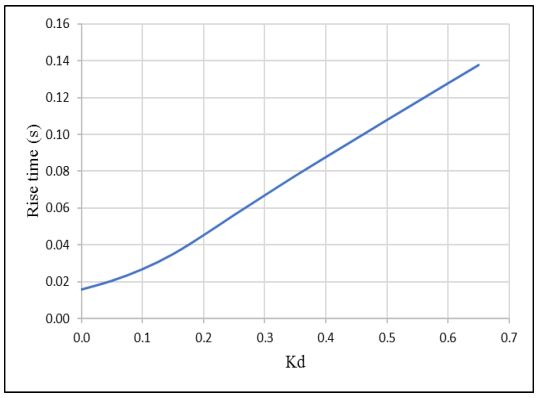

Figure 3.16: Rise time along derivative gain when proportional gain = 10

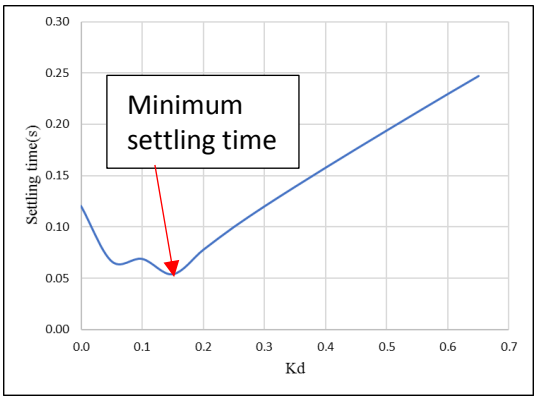

Figure 3.17: Settling time along derivative gain when proportional gain = 10

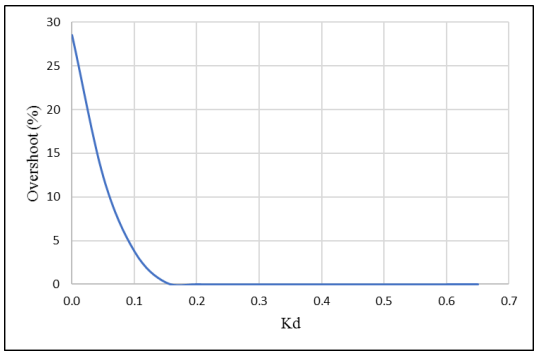

Figure 3.18: Overshoot along derivative gain when proportional gain = 10

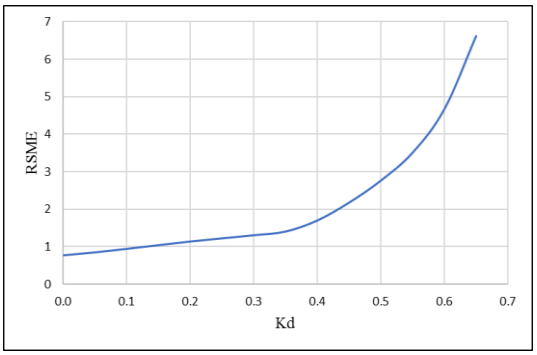

Figure 3.19: RMSE along derivative gain when proportional gain = 10

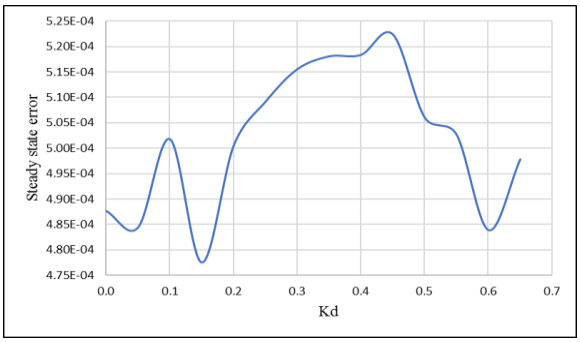

Figure 3.20: Steady-state error along derivative gain when proportional gain = 10

Table 3.5 shows the changes in step-response characteristics with gain variation in PD-LQR controller at Kp=10. The set data when Kd=0.15 gives the best overall performance of the system. Noted that the optimal derivative gain is differed for each proportional gain. Therefore, the process in determining the optimal derivative gain is repeated for every proportional gain by recording the step-response characteristics of the PD-LQR Simulink model in Microsoft Excel, plotting the graph and determining the optimal derivative gain for each proportional gain.

Table 3.5: Change in step-response characteristics with gain variation in PD-LQR controller at Kp=10

Kd	Rise time (s)	Settling time (s)	Overshoot (%)	RMSE	Steady State Error
0.00	0.016	0.120	28.500	0.775	4.88E-04
0.05	0.020	0.066	12.308	0.855	4.84E-04
0.10	0.027	0.069	3.759	0.949	5.02E-04
0.15	**0.035**	**0.054**	**0.223**	**1.046**	**4.78E-04**
0.20	0.045	0.078	0.006	1.144	5.01E-04
0.25	0.056	0.100	0.003	1.228	5.09E-04
0.30	0.067	0.120	0.001	1.311	5.16E-04
0.35	0.078	0.139	0.000	1.409	5.18E-04
0.40	0.088	0.158	0.001	1.705	5.18E-04
0.45	0.098	0.176	0.001	2.180	5.22E-04
0.50	0.108	0.194	0.002	2.766	5.06E-04
0.55	0.118	0.212	0.001	3.511	5.03E-04
0.60	0.128	0.229	0.002	4.669	4.84E-04
0.65	0.138	0.247	0.001	6.614	4.98E-04

Increment of Proportional Gain with Optimized Derivative Gain in PD-LQR

With the optimized derivative gain for each proportional gain, new graphs of the step-response characteristics along the proportional gain are plotted. Figure 3.21, Figure 3.22 and Figure 24 show the rise time, settling time and RMSE have the same trend as the proportional gain increases. The parameters decrease exponentially while having the minimum point at proportional gain=14. Figure 3.23 shows the overshoot of the system

experiences fluctuation between 0% to 2% as the proportional gain increases. Since the maximum overshoot is still under 10%, therefore the overshoot is not the deciding parameter in determining the optimal proportional gain. The steady-state error of the system showed in Figure 3.25 decreases exponentially and almost reaching a constant value as the proportional gain increases. Clearly, in determining the optimum proportional gain with the optimized derivative gain, the point that having the minimum settling time should be considered. The point with the minimum settling time also has the minimum rise time, minimum RMSE, low steady-state error and acceptable overshoot level.

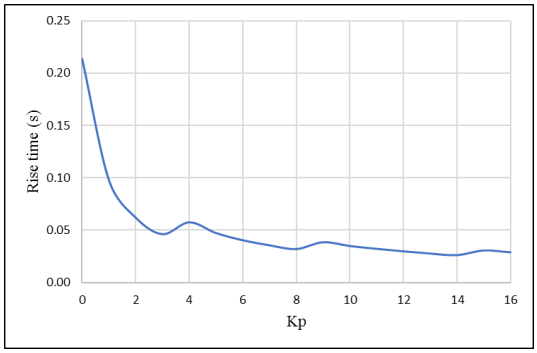

Figure 3.21: Rise time along proportional gain with optimized derivative gain

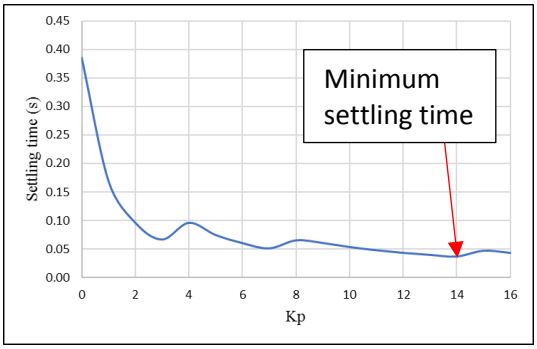

Figure 3.22: Settling time along proportional gain with optimized derivative gain

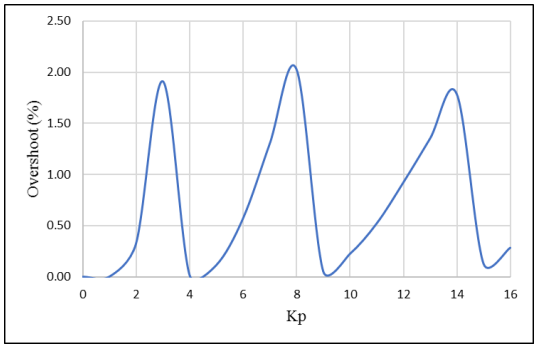

Figure 3.23: Overshoot along proportional gain with optimized derivative gain

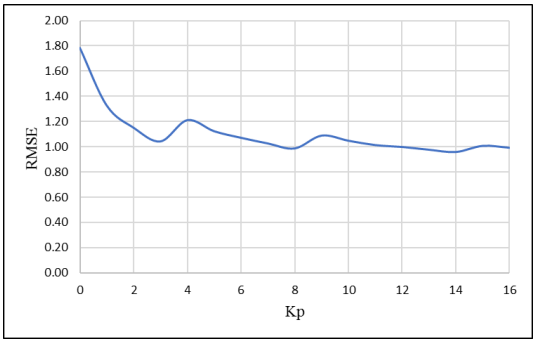

Figure 3.24: RMSE along proportional gain with optimized derivative gain

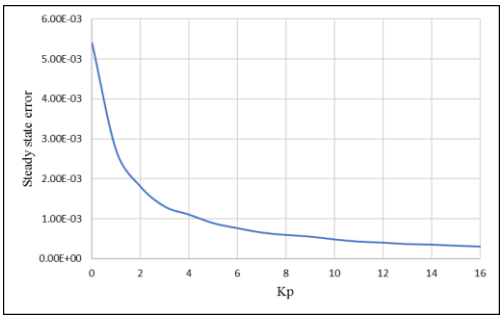

Figure 3.25: Steady-state error along proportional gain with optimized derivative gain

The tuning process can be improved by doing more iterations. The flow of the tuning process can be summarized in Figure 3.26. In this study, there are total of two iterations made in determining the optimum proportional gain. The number of iterations is limited due to the manual iteration made by using Microsoft Excel. The improvements in determining the derivative gain and proportional will be discussed in Chapter 5.

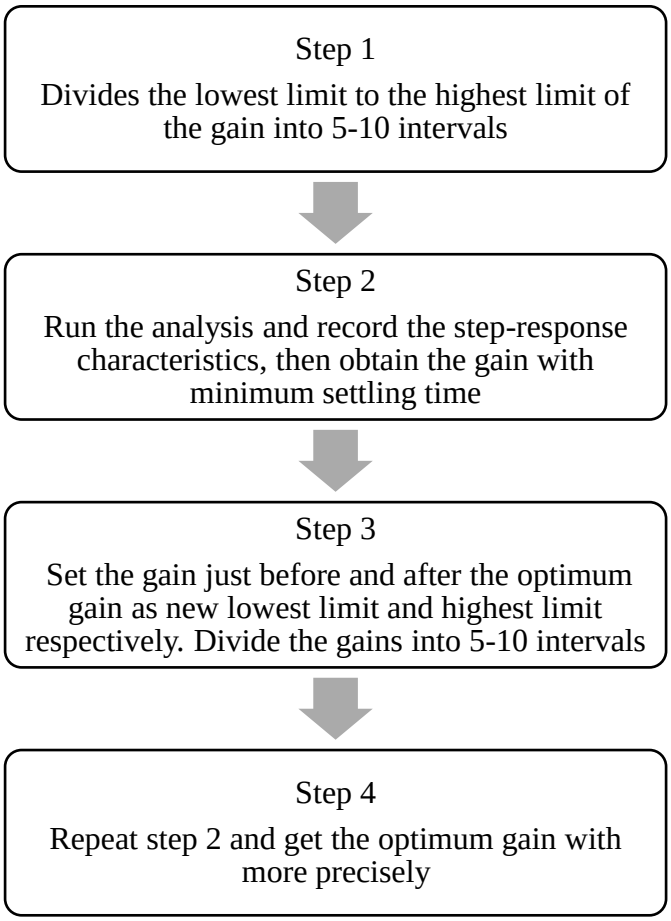

Figure 3.26: Flowchart for tuning derivative gain and proportional gain